

A spin metal-oxide-semiconductor field-effect transistor using half-metallic-ferromagnet contacts for the source and drain

S. Sugahara^{1,2} and M. Tanaka^{1,2}

¹*Dept. of Electronic Engineering, The University of Tokyo, 7-3-1 Hongo, Bunkyo-ku, Tokyo 113-8656, Japan*

²*PRESTO, Japan Science and Technology Agency, 4-1-8 Honcho, Kawaguchi, Saitama 332-0012, Japan*

We propose and theoretically analyze a novel metal-oxide-semiconductor field-effect-transistor (MOSFET) type of spin transistor (hereafter referred to as a spin MOSFET) consisting of a MOS gate structure and half-metallic-ferromagnet (HMF) contacts for the source and drain. When the magnetization configuration between the HMF source and drain is parallel (antiparallel), highly spin-polarized carriers injected from the HMF source to the channel are transported into (blocked by) the HMF drain, resulting in the magnetization-configuration-dependent output characteristics. Our two-dimensional numerical analysis indicates that the spin MOSFET exhibits high (low) current drive capability in the parallel (antiparallel) magnetization, and that extremely large magnetocurrent ratios can be obtained. Furthermore, the spin MOSFET satisfies other important requirements for "spintronic" integrated circuits, such as high amplification capability, low power-delay product, and low off-current.

Spin transistors, which utilize two ferromagnetic layers as a spin injector and a spin analyzer, possess unique output characteristics that are controlled by the relative magnetization configuration of the ferromagnets as well as the bias conditions¹⁻⁵. Also, the magnetization configuration in spin transistors can be used as nonvolatile binary data. Owing to these useful features, spin transistors are potentially applicable to integrated circuits for ultrahigh-density nonvolatile memory whose memory cell is made of a single spin transistor⁶ and for nonvolatile reconfigurable logic based on functional spin transistor gates⁷. In order to realize such "spintronic" integrated circuits with high performance, the following requirements must be satisfied for spin transistors; (i) large magnetocurrent ratio for nonvolatile memory and logic functions, (ii) high transconductance for high speed operation, (iii) high amplification capability (voltage, current and/or power gains) to restore propagating signals between transistors, (iv) small power-delay product and small off-current for low power dissipation, and (v) simple device structure for high degree of integration and high process yield.

Although various spin transistors have been proposed so far¹⁻⁵, none of them can satisfy all these requirements. Especially, the high transconductance and amplification capability cannot be realized simultaneously with the large magnetocurrent ratio. For example, large magnetocurrent ratios were reported in the spin-valve transistor proposed by Monsma et al² and spin transistors based on the similar operating

principle^{3,4}, however it is difficult for these devices to achieve high transconductance and high power gain due to the existing tradeoff between their transfer ratio and magnetocurrent ratio. On the other hand, the spin field-effect-transistor (FET) proposed by Datta and Dass⁵ can be expected to have high transconductance and high voltage gain, but its magnetocurrent ratio is limited to a very small value⁸.

In this paper, we propose and theoretically analyze a novel metal-oxide-semiconductor FET (MOSFET) type of spin transistor, hereafter referred to as a spin MOSFET, consisting of a MOS gate structure and half-metallic-ferromagnet (HMF) contacts for the source and drain. The proposed spin MOSFET can simultaneously satisfy all the above-described requirements (i)-(v) for spintronic integrated circuits.

Figure 1(a) schematically shows the device structure of the proposed spin MOSFET that can be applied to not only *n*-channel and *p*-channel devices but also accumulation- and inversion-type channel devices. The structure of the spin MOSFET is similar to that of Schottky source/drain MOSFETs^{9,10} except the HMF source/drain contacts that are the HMF/Si junctions without a *pn* junction. Possible candidates for the HMF materials are Heusler alloys, CrO₂, Fe₂O₃ and ferromagnetic semiconductors¹¹⁻¹⁴. Nonmagnetic (NM) contacts are also formed on the HMF source/drain (not shown in Fig. 1(a)). In the following, the *n*-channel accumulation-type spin MOSFET with an intrinsic Si channel layer is used to explain the operating principle of the spin MOSFET.

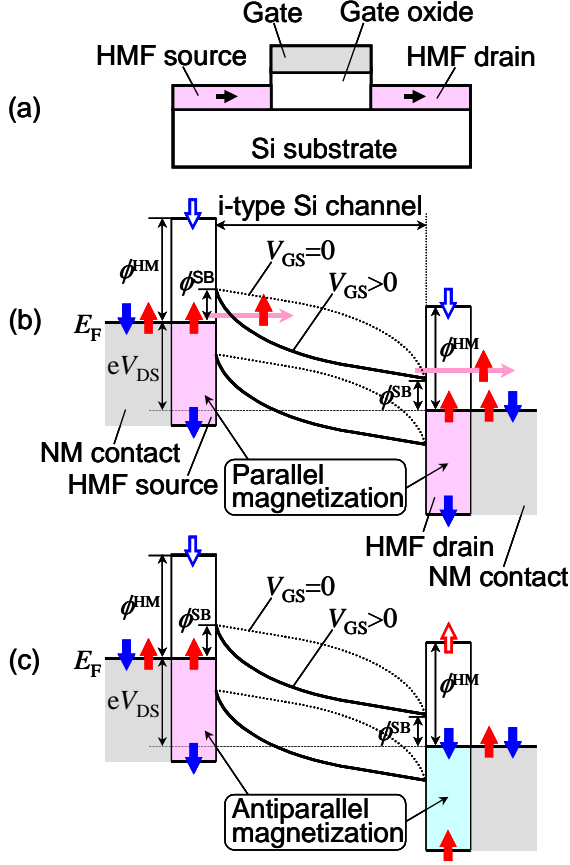


Fig. 1 Schematic (a) device structure and band diagrams of the spin MOSFET in (b) parallel and (c) antiparallel magnetization configurations.

Figure 1(b) schematically shows the band diagram of the spin MOSFET under a common source bias condition with and without a gate-source bias V_{GS} , where the relative magnetization configuration of the HMF source/drain is parallel. Owing to the metallic and insulating spin bands of the HMF source/drain material, spin-dependent barrier structures appear as shown in the figure, i.e., a Schottky barrier (SB) with a lower barrier height ϕ^{SB} for up-spin electrons and a rectangular energy barrier with a higher barrier height ϕ^{HM} for down-spin electrons (hereafter, this spin configuration at the HMF source is used throughout this paper). When a drain-source bias $V_{DS} (> 0)$ is applied with $V_{GS} = 0$, neither up-spin nor down-spin electrons are injected from the source to the channel due to the reverse-biased source-SB for up-spin electrons (as shown by the upper dotted curve in Fig. 1(b)) and the high rectangular barrier for down-spin electrons. By applying $V_{GS} (> 0)$, the width of the source-SB is reduced (as shown by the upper solid curve in the Fig. 1(b)) and thus up-spin electrons in the metallic spin band of the HMF source can tunnel

through the thinned source-SB into the channel. On the other hand, the injection of down-spin electrons is blocked even under the application of V_{DS} and V_{GS} owing to the high rectangular barrier at the source. Thus, the HMF source acts not only as a contact for blocking an off-current but also as a spin-injector of up-spin electrons from the HMF source to the channel. In the parallel magnetization configuration, the up-spin electrons injected in the channel can be transported to the nonmagnetic drain contact through the metallic up-spin band of the HMF drain, resulting in a drain current. By flipping the magnetization of the HMF drain, the antiparallel spin configuration is established and the HMF barrier height for up-spin electrons becomes larger at the drain, as shown in Fig. 1(c). Thus, the up-spin electrons hardly pass through the HMF drain to the nonmagnetic drain contact. Namely, the HMF drain has the function of a spin-analyzer, i.e., the HMF drain selectively extracts the up-spin electrons from the channel when the magnetic configuration between the HMF source and drain is parallel. By combining these spin-filter effects of the HMF source/drain, an extremely large magnetocurrent ratio can be expected due to the high spin-selectivity of the HMF source/drain.

A model device used in our analysis is shown in Fig. 2(a), where a thin-film-transistor structure was used for the simplicity of calculation. The size of this model device is as follows; the gate oxide (SiO_2) thickness t_{OX} is 2.0-3.0 nm, the Si layer thickness t_{Si} is 10 nm and the channel length L_{CH} is 30 nm. A device parameter L_S (L_D) shown in the figure is the distance from the source (drain) junction to the nonmagnetic contact, which qualitatively represents the thickness of the HMF source/drain shown in Fig. 1(a). An intrinsic Si layer was used for the channel and ballistic transport was assumed for the spin-polarized electrons injected in the channel. A relatively small SB height of $\phi^{SB} = 0.2$ eV for the metallic spin band of the HMF source/drain was taken in order to achieve a large drain current. A barrier height of $\phi^{HM} = 1.0$ eV for the rectangular barrier of the HMF source/drain and a distance of $L_S = 5$ nm ($= L_D$) were selected in order to obtain the fully spin-polarized electron injection from the HMF source¹⁵⁾. The effective mass m_{Si}^* of the Si layer used in the calculation was $0.19 m_0$, where m_0 is the free electron mass, and effective masses $m_M^* = m_0$ and $m_I^* = m_{Si}^*$ were assumed for the metallic and insulating spin bands of the HMF source/drain, respectively. The operating temperature was set at 300 K in all the calculations. Output

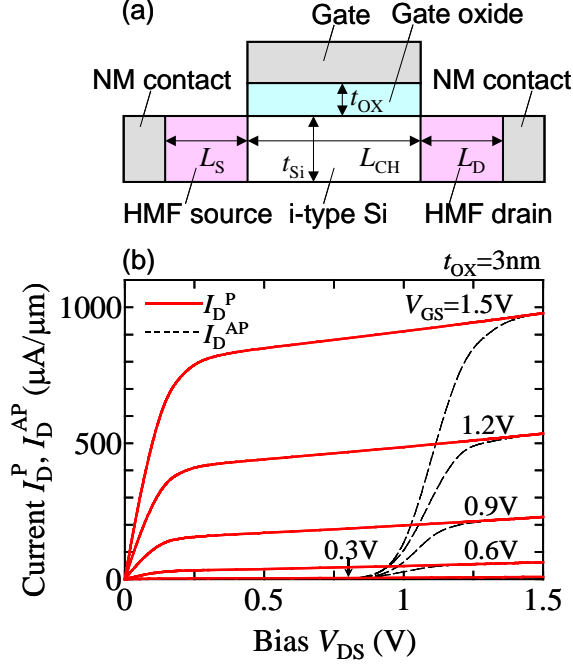


Fig. 2 (a) Device structure used for the analysis. The size of the device in our calculation is as follows; $t_{\text{OX}} = 2.0\text{-}3.0$ nm, $t_{\text{Si}} = 10$ nm, $L_{\text{CH}} = 30$ nm, and $L_{\text{S}} = L_{\text{D}} = 5$ nm. (b) Output characteristics of the spin MOSFET. The drain currents I_{D}^{P} (solid curves) and I_{D}^{AP} (dashed curves) in the parallel and antiparallel magnetic configurations, respectively, are plotted as a function of V_{DS} , where V_{GS} is varied from 0.3 to 1.5 V and t_{OX} is 3.0 nm.

characteristics were calculated by using the Tsu-Esaki formula¹⁶⁾ with a two-dimensional transmission probability calculation. The detailed calculation procedure will be described elsewhere¹⁵⁾.

Solid and dashed curves in Fig. 2(b) show the calculated output characteristics of the spin MOSFET for the parallel and antiparallel magnetization configurations, respectively, where t_{OX} is 3 nm. In the parallel magnetization, the drain current I_{D}^{P} starts to increase at V_{GS} more than 0.3 V (indicating the threshold voltage of 0.3 V) and increases nonlinearly with increasing V_{GS} , while I_{D}^{P} shows saturation behavior for V_{DS} . This output characteristics can be explained by the bias-induced potential profile of the channel region as follows: When V_{GS} and V_{DS} are applied simultaneously, V_{GS} induces a much stronger electric field from the gate electrode to the HMF source through the source-SB than that V_{DS} does from the drain to the source. Thus, the width of the source-SB for tunneling emission is thinned by V_{GS} as shown in Fig. 1(b) and it is insensitive to V_{DS} , resulting in the above

described output characteristics. The value of I_{D}^{P} is comparable to that of sub-100 nm scale MOSFETs¹⁷⁾, and I_{D}^{P} increases with decreasing the SB height (ϕ^{SB}) and gate oxide thickness (t_{OX}), like the conventional Schottky source/drain MOSFETs^{10,18)}. A large I_{D}^{P} more than $1500 \mu\text{A}/\mu\text{m}$ can be obtained for $\phi^{\text{SB}} = 0.2$ eV and $t_{\text{OX}} = 2.0$ nm with a gate bias condition of $V_{\text{GS}} = 1.5$ V. Note that reduction of t_{OX} is also important to obtain the saturation behavior of I_{D}^{P} , and the channel conductance of the spin MOSFET (discussed later) is improved by the reduction of t_{OX} .

In the antiparallel magnetization configuration, the drain current I_{D}^{AP} is negligibly small for V_{DS} less than $(\phi^{\text{HM}} - \phi^{\text{SB}})/e$ ($= 0.8$ V), but I_{D}^{AP} increases exponentially with increasing V_{DS} and reaches the same current value as I_{D}^{P} when V_{DS} is more than ϕ^{HM}/e ($= 1.0$ V), as shown in Fig. 2(b). Thus, magnetization-configuration-dependent output characteristics are realized when $V_{\text{DS}} < (\phi^{\text{HM}} - \phi^{\text{SB}})/e$. The exponential increase of I_{D}^{AP} can be attributed to the ballistic transport in the channel region, i.e., up-spin electrons injected from the HMF source can pass over the large rectangular barrier of the HMF drain when V_{DS} increases to more than $(\phi^{\text{HM}} - \phi^{\text{SB}})/e = 0.8$ V. Note that when the drain current is governed by drift-diffusion kinetics rather than ballistic transport, the exponential increase of I_{D}^{AP} is significantly suppressed. In this case, however, dynamically accumulated spin-polarized electrons in the channel would affect I_{D}^{AP} due to their finite spin lifetime for spin flipping. This effect can be treated by a self-consistent calculation based on a drift-diffusion model¹⁸⁾ including the spin lifetime, which will be reported elsewhere.

Figure 3(a) shows the magnetocurrent ratio γ_{MC} of the spin MOSFET as a function of V_{DS} at $V_{\text{GS}} = 1.5$ V, where γ_{MC} is defined by $(I_{\text{D}}^{\text{P}} - I_{\text{D}}^{\text{AP}})/I_{\text{D}}^{\text{AP}}$. γ_{MC} exponentially falls with increasing V_{DS} , since I_{D}^{AP} increases exponentially with increasing V_{DS} when V_{DS} is less than ϕ^{HM}/e as described above. In spite of this bias-dependence, extremely large γ_{MC} more than 1000 % can be obtained for V_{DS} less than 1.0 V. To obtain even larger γ_{MC} , higher ϕ^{HM} values are required. It should be noted that when the drift-diffusion transport is dominant, this strong bias-dependence of γ_{MC} is significantly suppressed and extremely large γ_{MC} will be obtained even at $V_{\text{DS}} = 1.5$ V.

The results shown in Figs 2(b) and 3(a) indicate that the spin MOSFET possesses the magnetization-configuration-dependent output characteristics with large γ_{MC} . Thus, the spin MOSFET satisfies the above-mentioned requirement

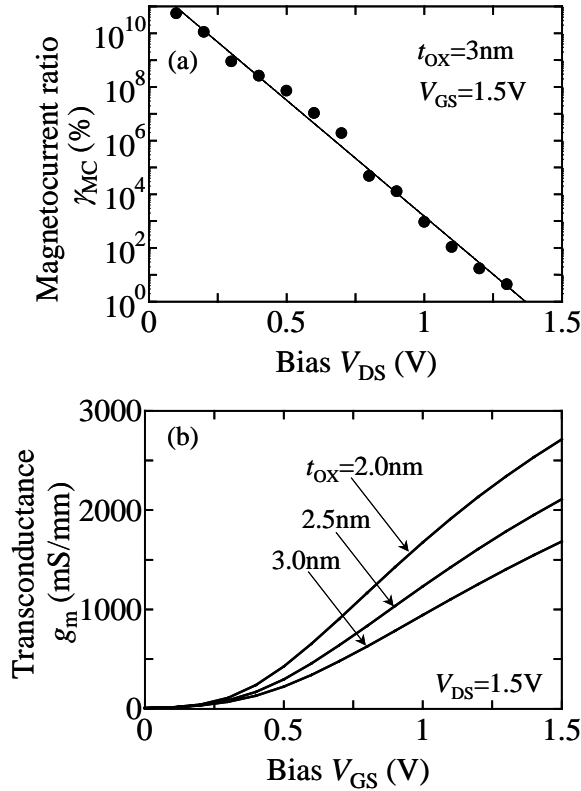


Fig. 3 (a) Magnetocurrent ratio $\%MC$ [= $(I_D^P - I_D^{AP})/I_D^{AP}$] as a function of V_{DS} at $V_{GS} = 1.5\text{ V}$. (b) Transconductance g_m ($= \partial I_D^P / \partial V_{GS}$) as a function of V_{GS} at $V_{DS} = 1.5\text{ V}$ for $t_{OX} = 2.0, 2.5$ and 3.0 nm .

(i) for spintronic integrated circuit applications. The other requirements were examined by the on- and off-current characteristics of the spin MOSFET as follows: Figure 3(b) shows the transconductance g_m of the spin MOSFET in the parallel magnetization configuration as a function of V_{GS} at $V_{DS} = 1.5\text{ V}$, where t_{OX} is varied from 2.0 to 3.0 nm. Here, g_m is defined by a derivative $\partial I_D^P / \partial V_{GS}$ under a fixed V_{DS} condition, which is a measure of the output-current (I_D^P) drive capability for the input voltage (V_{GS}). Since I_D^P increases nonlinearly ($I_D^P \propto F^2 \exp(-1/F)$) with increasing the strength F of the electric field through the source-SB¹⁰⁾, g_m increases with increasing V_{GS} and with decreasing t_{OX} as shown in Fig. 3(b). A large g_m of 1000 mS/mm, which is comparable to (or larger than) that of sub-100 nm scale MOSFETs¹⁷⁾, can be obtained at $V_{GS} = 1.0\text{ V}$ for $t_{OX} = 3\text{ nm}$, and g_m is further enhanced to more than 1500 mS/mm by reducing t_{OX} to 2 nm, as shown in the figure. These large g_m values of the spin MOSFET lead to a small propagation delay t_{pd} and a large voltage gain G_V , since t_{pd} and G_V can be estimated by C_L/g_m and

g_m/g_D , respectively, where C_L is a load capacitance including a parasitic capacitance and g_D is a channel conductance given by a derivative $\partial I_D^P / \partial V_{DS}$.

Furthermore, the large g_m of the spin MOSFET enables low-voltage operation, and the voltage swing can be less than 1.0 V. This results in a small power-delay product $P \cdot t_{pd}$ (that corresponds to the energy per switching), since this energy is proportional to the square of the voltage swing¹⁹⁾. The power dissipation is also caused by the off-current in the stand-by condition of the spin MOSFET, which is characterized by the subthreshold swing S calculated from $\log I_D^P - V_{GS}$ characteristics. Although S depends on t_{OX} and it decreases with decreasing t_{OX} , S can take $\sim 200\text{ mV/decade}$ for $t_{OX} = 2\text{ nm}$, implying a relatively small off-current. Note that S can be reduced remarkably by increasing ϕ^{SB} , although there exists a tradeoff between I_D^P and S because I_D^P decreased with increasing ϕ^{SB} .

Since the spin MOSFET presented here has the excellent performance in sub-100 nm regime and it has a simple structure as shown in Fig. 1(a), one can expect the scaling merits by downsizing the spin MOSFET and high degree of integration. Therefore, the spin MOSFET satisfies all the requirements (i)-(v) for spintronic integrated circuit applications.

In summary, we have proposed and theoretically analyzed the spin MOSFET with HMF source and drain. The spin MOSFET was shown to have magnetization-dependent-output characteristics, high transconductance, amplification capability, low power-delay product, low off-current, and a simple structure compatible with Si-MOS technology, which are all important for integrated circuit applications. The spin MOSFET can be used as a key device for ultrahigh density nonvolatile memory and reconfigurable logic devices based on novel spintronic concepts.

Acknowledgement

This work was supported by the PRESTO program of JST, a Giant-in-Aid for Science Research on the Priority Area "Semiconductor Nanospintronics" (14076207), the IT program of RR2002 from MEXT, and Toray Science Foundation.

References

- 1) M. Johnson, Phys. Rev. Lett. 70 (1993) 2142.
- 2) D.J. Monsma, J.C. Lodder, Th.J.A. Popma and B. Dieny, Phys. Rev. Lett. 74 (1995) 5260.
- 3) K. Mizushima, T. Kino, T. Yamaguchi and K.

- Tanaka, IEEE Trans. on Magnetism 33 (1997) 3500.
- 4) S. van Dijken, X. Jiang and S.S.P. Parkin, Appl. Phys. Lett. 80 (2002) 3364.
 - 5) S. Datta and B. Das, Appl. Phys. Lett. 56 (1990) 665.
 - 6) S. Sugahara and M. Tanaka, The 9th Symp. on the Physics and Applications of Spin-related Phenomena in Semiconductors, Tokyo, 2003, D5.
 - 7) T. Matsuno, S. Sugahara and M. Tanaka, The 9th Symp. on Physics and Applications of Spin-related Phenomena in Semiconductors, Tokyo, 2003, D6.
 - 8) C.M. Hu, J. Nitta, A. Jensen, J.B. Hansen and H. Takayanagi, Physica E 10 (2001) 467.
 - 9) T. Lepselter and S.M. Sze, Proc. IEEE 56 (1968) 1400.
 - 10) R. Hattori and J. Shirafuji, Jpn. J. Appl. Phys. 33 (1994) 612.
 - 11) R.A. de Groot, F.M. Mueller, P.G. van Engen and K.H.J. Buschow, Phys. Rev. Lett. 50 (1983) 2024
 - 12) A. Yanase and K. Shiratori, J. Phys. Soc. Jpn. 53 (1984) 312.
 - 13) K. Schwarz, J. Phys. F16 (1986) L211.
 - 14) K. Sato and H. Katayama-Yoshida, Semicond. Sci. Technol. 17 (2002) 367.
 - 15) S. Sugahara and M. Tanaka, in preparation.
 - 16) R. Tsu and L. Esaki, Appl. Phys. Lett. 22 (1973) 562.
 - 17) H. Iwai, Microelectronics Journal 29 (1998) 671.
 - 18) W. Saito, A. Itoh, S. Yamagami and M. Asada, Jpn. J. Appl. Phys. 38 (1999) 6226.
 - 19) J.A. Cooper, JR., Proc. IEEE 69 (1981) 226.